

RESEARCH ARTICLE

A geomagnetic bio-inspired homing method based on diversity-first search strategy

Kun Liu^{1,*}, Ying Lei², Wenna Fan¹

¹School of Electronic Engineering, Xi'an Aeronautical Institute, Xi'an, Shaanxi, China. ²School of Mechanical & Electrical Engineering, Xi'an Traffic Engineering Institute, Xi'an, Shaanxi, China.

The uncertainty in the process of geomagnetic bio-inspired homing, caused by limitations in field measurement of the geomagnetic field, introduces randomness into the homing time. While this random characteristic aligns with animal homing behavior, it hinders the practical application of geomagnetic bionic homing. The proposed bionic homing search method based on diversity priority aimed to enhance the directional behavior of homing by augmenting the diversity within the evolutionary population, thereby curbing non-directional drift in response to changes in the homing path. The generation mechanism of geomagnetic bionic homing uncertainty was analyzed in this study. A homing search strategy prioritizing diversity was then proposed. Subsequently, a diversity measurement method based on behavioral entropy was constructed and an accompanying homing algorithm was provided. The effectiveness of the proposed method was verified through digital simulation and analysis.

Keywords: homing method; geomagnetic bio-inspired navigation; searching strategy; multi-objective optimization.

*Corresponding author: Kun Liu, School of Electronic Engineering, Xi'an Aeronautical Institute, Xi'an 710077, Shaanxi, China. Email: 201904017@xaau.edu.cn.

Introduction

The geomagnetic field serves as the inherent coordinate system of nature, and its numerous characteristic parameters establish a direct correspondence with the near-earth space, rendering it a dependable source of information for long-distance migration, navigation, homing, and other navigational behavior [1-3]. The study investigates the navigation method of geomagnetic bio-inspired homing, which draws inspiration from animal homing behavior utilizing the geomagnetic field and does not rely on a pre-existing database [4, 5].

Homing behavior is a widespread phenomenon in the natural world. It has been demonstrated that certain animals such as turtles, homing pigeons, and salmon possess the ability to

perceive the magnetic field characteristics of their nests and birthplaces through a process known as 'imprinting [6, 7]. These animals rely on their perception of magnetic field parameters to navigate back to their destinations even after traversing vast oceans or covering thousands of kilometers. In the process, it would be hard to imagine if their simple brains could record a complete map of the geomagnetic distribution. To reveal this amazing behavioral phenomenon, scholars have done a lot of research. With the help of satellite technology, scientists analyzed the geomagnetic data characteristics of long-distance migratory animals and confirmed that the change of migration route was related to the change of magnetic field [8]. With the help of comparative analysis, the phenomenon and ability of biological homing using magnetic field are confirmed [1, 2, 9]. As the sensing organ of

magnetic field in animals, magnetic receptors have been found in a variety of organisms [10, 11], which further confirms that animals have the ability of magnetic navigation. Monteil *et al.* demonstrated the existence of a priori geomagnetic database in the biological brain [12]. In the field of geomagnetic homing modelling, it is still mainly based on assumptions and conjectures, which is in its infancy. Winklhofer proposed the biomimetic navigation model of map and compass, in which the magnetic field was controlled by living beings [13]. Dora assumed that the magnetic field parameter distribution changed linearly and proposed a predictive navigation model [14]. According to historical data, the magnetic field distribution in the unreached area can be inferred to realize the purpose of navigation. There are two disadvantages to the two methods described above. One is that the calculated homing route is certain and unique, which does not conform to the natural biological path. Second, the influence of abnormal magnetic field on homing cannot be overcome. Previous studies regarded the magnetic field parameters as approximate linearization and used the dynamic estimation method to calculate the homing route [15, 16]. This method could obtain a clear homing route in the area with slow magnetic field change, but it was difficult to deal with the area with complex magnetic field change and abnormal magnetic field. Researchers constructed a biomimetic homing model based on multi-objective search, which was proposed from the perspective of biological multi-parameter perception of magnetic field. The idea of evolutionary search was used to obtain the navigation path [5, 17]. This method had strong robustness and could overcome the influence of magnetic field anomaly on homing behavior through behavioral constraints. However, the uncertainty of this method was obvious, and the search time was random.

To solve the above problems, inspired by the migration behavior of sea turtles, we proposed a diversity-first geomagnetic biomimetic homing method with the help of the idea of evolutionary

search to track the navigation solution. Through this study, the mechanism of the uncertainty of homing time was analyzed, and the influence of each evolutionary operation on population drift was clarified. In addition, the diversity priority search strategy was given from the perspective of population migration and the dynamic change of homing solution. Further, based on the TES homing algorithm, a diversity priority homing search algorithm was designed. The effectiveness and rationality of the proposed algorithm were verified by simulation analysis.

Materials and methods

Geomagnetic bionic homing

Geomagnetic field is the inherent field of the earth, which has a variety of characteristic parameters. It is a natural navigation information source in nature and provides reliable navigation clues for many animals. In the context of no prior geomagnetic database, the homing process of animals starting from any point k on the surface to the established destination T by using the perception of magnetic field changes can be summed up as the process of convergence of multiple parameters of the geomagnetic field to their respective goals according to the homing path (MOMP) with the help of the multi-objective theory. Without loss of generality, it is characterized as follows.

$$\begin{cases} \min F(\mathbf{B}, k) = (f_1(B_1, k), f_2(B_2, k), \dots, f_n(B_n, k))^T \\ s. t. G(\mathbf{B}, k, u) \end{cases} \quad (1)$$

where, k was the magnetic field feature set at any position. n was the dimension of the geomagnetic field. $\mathbf{B}^k = \{B_1^k, B_2^k, \dots, B_n^k\}$. Since no geomagnetic map was established in the search process, and the homing behavior did not depend on the change of geographical position, the location label could be regarded as the search time label. G was the path constraint function, which was composed of the magnetic field parameter set \mathbf{B} , the search behavior u and k . At the time with $\mathbf{B}^k = \mathbf{B}^T$, the function F achieved

the minimum value, *i.e.*, the carrier reached the target point T. From the perspective of multi-objective optimization, through the perception of the surrounding magnetic field environment at different times, the Pareto solution set satisfying equation (1) could be obtained by the carrier. Connecting the Pareto solution sets at consecutive times could form a homing path connecting the starting point and the ending point as shown in Figure 1.

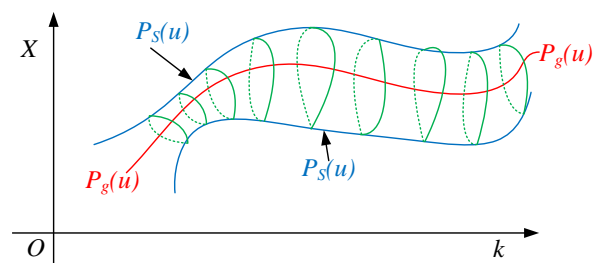


Figure 1. Dynamic distribution diagram of spatial solutions.

$P_g(u)$ was the optimal solution and $P_s(u)$ was the boundary of Pareto solution. Affected by the distribution of magnetic field parameters, the range and gradient direction of Pareto solution changed with time. In the actual process of homing, due to limitations in the magnetic field measurement method, the carrier's perception of changes in magnetic field parameters was posteriori in nature. Only after the carrier moved itself and generated corresponding positional changes, it could obtain information about magnetic field changes along its moving direction. However, the carrier's motion capability was preferred, and the distribution of magnetic field parameters outside the homing path remained unknown. When $P_g(u)$ changed, the carrier failed to promptly respond to dynamic variations in the solution curve, thereby risking loss of tracking accuracy.

Homing search strategy with diversity priority

In the case of limited ability of magnetic field sensing and environmental exploration, using the idea of population evolution to conduct

geomagnetic homing search is undoubtedly an excellent homing strategy.

1. Uncertainty analysis in homing

In the process of homing, the search behavior was used to construct the population sample. The path constraint function G was used as the sample evaluation function, and the evolutionary population was sequentially evolved by executing the population sample. Considering the population size as N_{pop} , each possible population distribution was regarded as a state, and $S_{pop}(k)$ represented the population sample distribution state at time k . All possible population states formed the finite state space A , whose cardinal number was $|A| = 2^{N_{pop}}$. Obviously, A was a finite state space. The evolutionary process of each generation in a population is considered as a transfer process from one state to another, which is achieved through the operator of reproduction, elimination, and mutation. Let the state transition matrix of replication operation, elimination operation, and mutation operation be R , E , and M , respectively. At the time $k \rightarrow k + 1$, the population state transition could be represented by equation (2).

$$S_{pop}(k+1) = \begin{cases} \mathbf{M} \cdot \mathbf{R} \cdot (S_{pop}(k)) & G \leq 0 \\ \mathbf{M} \cdot \mathbf{E} \cdot (S_{pop}(k)) & G > 0 \end{cases} \quad (2)$$

Among them, at $k + 1$, the population stated $S_{pop}(k + 1)$ two transfer processes based on the evaluation results of the sample using the taxis constraint function G . If $G \leq 0$, a new state $S_{pop}(k + 1)$ was obtained by replicating R and mutating M from the previous state $S_{pop}(k)$. On the other hand, if $G > 0$, a new state $S_{pop}(k + 1)$ was obtained by eliminating E and mutating M from the previous state $S_{pop}(k)$.

(1) Reproduction operator

The reproduction operator transfers the population from one state to another by replicating high-quality samples and increasing the distribution probability of high-quality samples. The transfer process described herein

was a directed transfer, constrained by the fitness of the samples, which facilitated the convergence of population samples towards high-quality ones. This phenomenon could be denoted as $S(x) \rightarrow S^*(x)$. After multiple replication operations, the high-quality individuals in Pareto solution set would gradually occupy the evolutionary population, making their sample probability tend to 1. In other words, the reproduction operation facilitated the convergence of the population towards samples with higher fitness, thereby establishing a distinct directional movement pattern within the search space. At the same time, the rate of population state transfer was affected by the depth of replication. The high transfer speed could facilitate population convergence towards the optimal solution, yet it might also lead to premature convergence of the population. Once the optimal solution changed, the phenomenon of population drift would occur. In other words, the replication operation helped the evolutionary population to reach the mature state S^* , but when the solution curve changed and the optimal solution x^* was not in the population, the replication operation alone could not make the population entering the new mature state S'^* . In this case, S^* and S'^* were not connected, *i.e.*, the algorithm lacked dynamic search capability.

(2) Elimination operator

The elimination operator is an evolutionary operation related to fitness evaluation results. It generates new individuals by means of undirected transfer, and promotes the undirected transfer of population states, so as to facilitate the interworking between different states. The intercommunication ability was independent of the initial state of the population. However, the elimination operator has a relatively limited role in promoting population intercommunication, mainly because the selection of optimal samples can inhibit the effects of culling operations. At the onset of the search, the elimination operation can facilitate a breadth-first exploration by providing more comprehensive insights into the environment. However, once an optimal solution is obtained at

a given time, the population tends to converge towards that sample, thereby increasing the likelihood of distribution bias towards optimal solutions. Consequently, samples with lower fitness values gradually diminish, leading to reduced occurrences of elimination operations and indirectly attenuating their impact on inter-state interactions within the population. The elimination operation is an evolutionary process closely associated with the evaluation of fitness, which facilitates the generation of novel individuals through undirected transfer and readily influences the overall population dynamics.

(3) Mutation operator

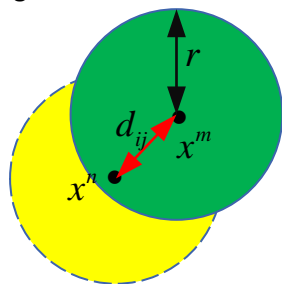
To facilitate intercommunication among the population states, the introduction of mutation operators is very necessary. The mutation operator acts on the individual of the population independently and causes the individual to produce variation in the form of equal probability, causing the population state to shift aimlessly. From two perspectives, on one hand, the mutation operator employs an undirected approach to generate novel samples, promoting population divergence and facilitating inter-population communication. On the other hand, it impedes population convergence, potentially resulting in a gradual degradation of the trend characteristics of evolutionary methods and entering a stochastic search stage that reduces algorithmic convergence speed. Considering the population state transfer perspective, we analyzed the action mechanism of each relevant operation on population drift. Among them, the replication operator represented a directional operation that facilitated convergence of the population towards a specific absorption state and effectively reduced population diversity, which was a key factor contributing to population drift. On the other hand, elimination and mutation operators represented astatic operations that generated new sample individuals, thereby enhancing its diversity, and mitigating the occurrence of population drift. However, while the replication operation served as primary driver of population drift, it also

played a crucial role in promoting algorithm convergence. Conversely, the elimination and mutation operations facilitated intercommunication among population states but might impede the speed of algorithm convergence. To strike a balance between suppressing population drift and ensuring optimal search performance, effective coordination among these three evolutionary operations was essential.

2. Population drift suppression strategy

The analysis in the preceding section revealed a strong correlation between the emergence of population elegance and population diversity. Consequently, a Diversity First (DF) based strategy for suppressing population drift was designed while ensuring algorithm convergence. Assuming that, in the homing process, x_i^n and x_j^m denoted the optimal solutions x^n at time i and x^m at time j , respectively, a behavior distance $d_{ij}(x^n, x^m)$, denoted as d_{ij} , where r represented the radius of the region occupied by the containing absorption state.

a. Internal migration



b. External migration

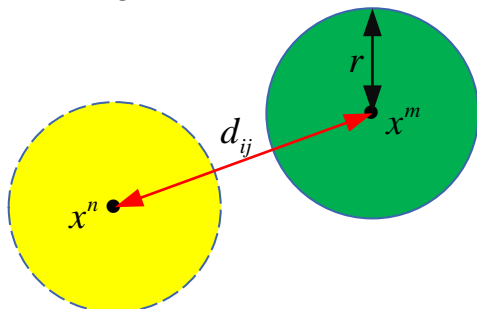


Figure 2. Schematic representation of population sample migration mechanism.

The internal migration was illustrated in Figure 2a, where the distance d_{ij} between x^n and x^m was smaller than the radius of the attraction domain r , indicating that x^m fell within the existing state $S(i)$. On the other hand, Figure 2b depicted external migration, characterized by $d_{ij} > r$ and exclusion of x^m from the existing state $S(i)$, thus making it a new sample type. In the case of internal migration as depicted in Figure 2a, where the population included x^m , the transfer process from state $S(i)$ to $S(j)$ could be achieved through directional transfer with a transfer probability denoted as $P_s(j|i)$. Conversely, for external migration illustrated in Figure 2b, where x^m was not presented in the population, the transfer process from state $S(i)$ to $S(j)$ could only occur with a certain probability if x^m was regenerated, and this probability was denoted as $P'_s(j|i)$. According to the analysis results, $P_s(j|i)$ exhibited significantly higher values compared to $P'_s(j|i)$. Expanding the range of the attractive domain emerged as one of the most intuitive approaches for enhancing $P_s(j|i)$. By enlarging the radius r of the attraction domain, it became possible to accommodate a larger population x^m , thereby transforming external migration into internal migration and increasing the transfer probability $P_s(j|i)$. However, an indiscriminate increase in r might lead to population divergence, impeding algorithm convergence speed, and prolonged homing search time. Therefore, considering a moderate expansion of the radius, acceptable homing time constraints could facilitate completion of transfer processes within a single attraction region as much as possible and effectively inhibit population drift. In addition, the convergence rate of the algorithm could also be considered as an indicator of population diversity change. The migration rate of the population represented the change rate of population diversity, and rapid drift facilitated the rapid convergence of the population towards a new attractor region. However, due to complex and unknown background factors, deceptive issues might arise during this process. It should be noted that the new attractor kernel did not necessarily represent the optimal solution, which

often led to local convergence dilemmas. The slow drift speed, however, prolonged the existence of the old attraction domain, hindering timely tracking of solution curve changes by the algorithm and thereby impacting its long-term performance. To address this issue, it is necessary to consider the rate of change in population diversity.

Results and discussion

Algorithm of geomagnetic bio-inspired homing

A geomagnetic bio-inspired homing algorithm based on TES-DF was designed by introducing DF population drift suppression strategy based on TES homing algorithm [5]. The distribution entropy was utilized for quantifying population diversity, and a correlation between the distribution entropy and the attraction area radius was established. Building upon a fundamental bionic navigation algorithm and DF suppression strategy, an enhanced bionic navigation algorithm based on TES-DF was proposed, accompanied by a detailed description of its workflow.

Diversity measurement based on behavioral entropy

At present, diversity has received extensive attention in the performance research and construction of evolutionary algorithms [18-20]. However, the quantitative description of diversity is relatively few. Most studies describe population diversity by measuring the location differences of sample individuals in multiple spatial dimensions, which has some shortcomings in population search ability and attraction domain scale description. In general, the diversity obtained when individuals are far away from the majority is similar to the diversity obtained when the majority is dispersed. For these reasons, distribution entropy was introduced here to describe the diversity of population quantitatively. Distribution entropy is defined as that, assuming that the class of behavior is M , each behavior can be expressed as u_1, u_2, \dots, u_M . At a certain moment in a group of

evolution, the ratio of all kinds of behavior in group respectively as $P(u_1), P(u_2), \dots, P(u_M)$, satisfy the $\sum_{i=1}^M P(u_i) = 1$. Thus, distribution entropy H can be defined as:

$$H(P(u_1), P(u_2), \dots, P(u_M)) = -\sum_{i=1}^M P(u_i) \ln P(u_i) \quad (3)$$

where H is a strictly concave function with non-negative, symmetric and additive properties in distribution space. The distribution entropy H describes population diversity from the perspective of behavior types. The distribution probability of each behavior in the population is directly reflected by the level of distribution entropy. Especially in the real value evolution algorithm similar to taxis evolution, the number of species of behavior samples determines the size of the attractive field of the population: when the sample type of the population is single, the distribution entropy $H \rightarrow 0$ the population diversity is the lowest, and the radius of the attractive field is the smallest. When the distribution probability of each sample in a population is similar, the distribution entropy H is the largest, the population diversity is the highest, and the radius of the attraction domain is the largest. In addition, the rate of change of population diversity can be characterized by the first derivative of distribution entropy H .

The algorithm of TES-DF homing

Based on TES navigation algorithm, in the homing search process, based on the value of H , the corresponding evolution operator was used to regulate the population diversity, so as to achieve the purpose of inhibiting population drift and reducing search uncertainty.

The homing algorithm based on TES-DF was designed as follows:

(1) Step0 Initialization:

Initializing the population $Pop(0)$, loading the geomagnetic environment B^T of the target point, and obtaining the magnetic environment B^0 at the initial position through field measurement.

(2) Step1 Terminate the decision:

Calculating the multiple objective function F , if $F < \sigma$, then terminating the homing. Otherwise, going to Step2.

(3) Step2 Homing search:

Selecting q_i with randomly, and performing homing search, then measuring the current geomagnetic field parameter B^k .

(4) Step3 Evaluate sample performance:

Calculating the fitness function $G(k)$, if $G(k) \leq 0$, going to Step4. Otherwise, going to Step5.

(5) Step4 Reproduction operator:

Executive reproduction operator, going to step6.

(6) Step5 Elimination operator:

Executive elimination operator, go to Step6.

(7) Step6 Mutation operator:

Executive Mutation operator.

(8) Step7 Threshold entropy H_{th} determination:

Calculating the population distribution entropy H . And then, if $H \geq H_{th}$, executing in sequence. Otherwise, increasing the entropy of population distribution and going to Step1.

(9) Step8 Distribution entropy H regulation:

Going to Step1.

The effectiveness of the bio-inspired homing algorithm

The effectiveness of the bio-inspired homing algorithm based on TES-DF proposed in this paper was verified by utilizing the international geomagnetic model IGRF-13 to construct the homing background field and conducting simulation verification in MATLAB. Assuming that the carrier was a particle, the step size in unit time was $L = 500$ m, and the accuracy of the carried magnetic sensor was 0.1 nT and 0.1° . Other parameters were set as $D_\theta = 30^\circ$, $N_{pop} = 50$, $N_{spr} = 1$, and $p_{mut} = 0.02$.

(1) Comparative analysis of homing effect

The performance of different algorithms was compared between TES and TES-DF within MATLAB. With the same homing task as the background, the minimum threshold entropy $H_{th} = 1.3$, population size $N_{pop} = 50$, sampling interval $D_\theta = 30^\circ$, replication depth $N_{spr} = 4$, mutation probability $P_{mut} = 0.01$ were set to conduct simulation experiments. In the homing route of TES algorithm, point "O" represented the carrier homing starting position, point "T" represented the homing target position (Figure 3).

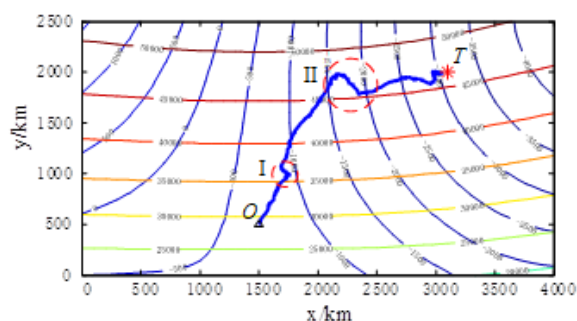


Figure 3. The homing route of TES algorithm.

The magnetotaxis intensity change during the homing process was shown in Figure 4. The time period between the dashed boxes of 'I' and 'II' corresponded to the zigzag area 'I' and 'II' that appeared in the homing route in Figure 3. In combination with Figure 4, before entering 'I' and 'II', the magnetotaxis intensity reached or even exceeded 45, at which time the population was already in the mature state. However, due to the change of the solution curve, the drift phenomenon appeared in the evolved population. In order to transition into a new mature state, the evolving population must intensify its exploration of the environment and reduce its magnetotaxis intensity in order to acquire a fresh optimal solution and regain maturity. This iterative search process visually demonstrated the convoluted nature of the homing path, with its complexity directly linked to the challenge of reattaining an optimal solution as search difficulty increasing, so did the

tortuosity of the homing path. It was evident that population drift-induced re-search not only prolonged unnecessary homing time but also heightened the risk of failed navigation searches due to difficulties in obtaining an optimal solution. Clearly, it was imperative to suppress population drift. It should be noted that multiple instances of population drift might occur during the homing process. However, these instances were minor and could be swiftly resolved as populations migrate towards a new mature state without reaching levels of path tortuosity seen in areas 'I' and 'II' depicted in Figure 3.

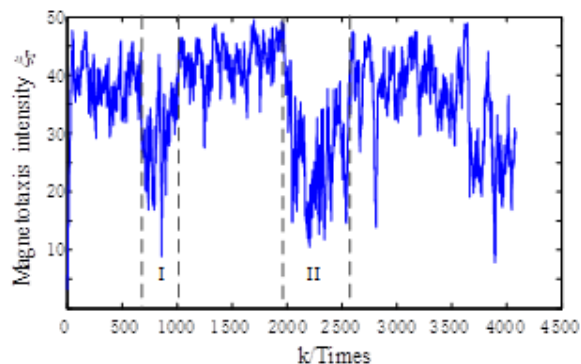


Figure 4. Magnetotaxis intensity change in the homing process of TES algorithm.

The homing route of TES-DF algorithm was depicted in Figure 5. In order to ensure successful homing, the motion path exhibited only a few minor deviations and twists. The magnetotaxis intensity change during the homing process of Figure 5 was illustrated in Figure 6. By setting a threshold entropy, the magnetotaxis intensity ξ_T was constrained to be within 45, with ξ_T ranging between 25 and 40 for most of the time. During the zigzag part shown in Figure 5, the magnetotaxis intensity ξ_T fell within the range of 15 and 30. In the process of TES-DF homing with DF suppression strategy, the radius r of population attraction domain was increased by setting a threshold entropy. This approach enabled the population to retain a wider range of sample types and reduced the complexity of discovering new optimal solutions. After the

population drift appeared, the migration of population samples was made as internal migration as possible, which shortened the time-consuming of population re-search, and then improved the efficiency of homing. In the overall homing movement, the number and degree of path tortuosity were significantly improved.

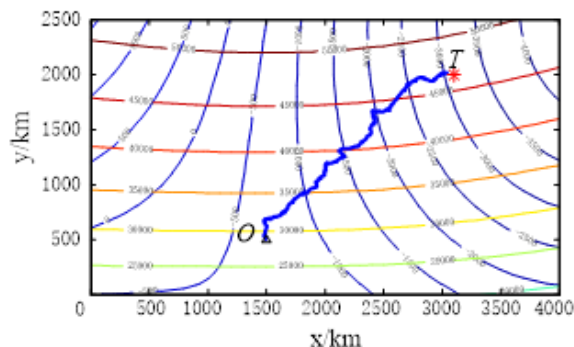


Figure 5. The homing route of TES-DF algorithm.

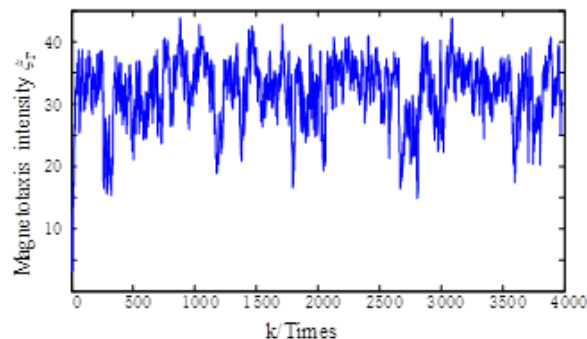


Figure 6. Magnetotaxis intensity change in the homing process of TES-DF algorithm.

(2) Comparative analysis of homing time

The single homing result was difficult to fully reflect the overall performance of the algorithm, so we conducted multiple homing experiments and used the statistics of homing time to analyze the performance of the algorithm. A certain position in space was randomly selected as the target point, and five starting points were set around the position to carry out the homing test, which was called task i ($i = 1, 2, \dots, 5$). For five tasks, TES homing algorithm and TES-DF homing algorithm were used respectively to conduct

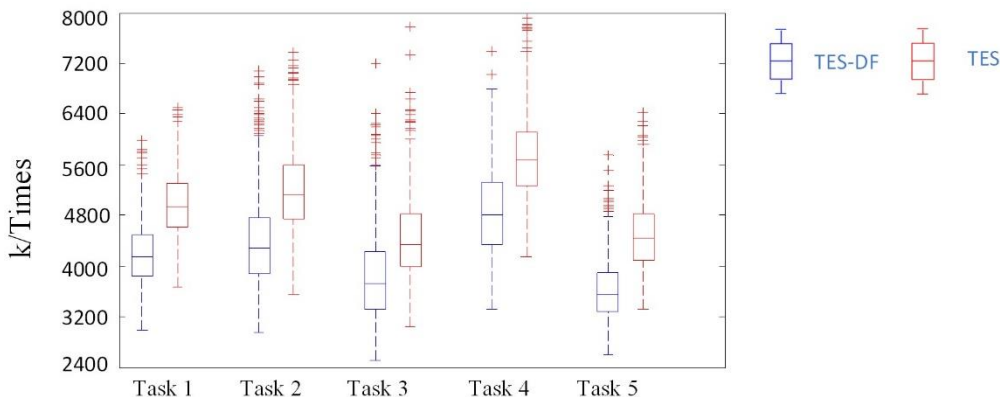


Figure 7. Box plot of homing time.

comparative analysis experiments. The results were shown in Table 1 and Figure 7, respectively.

Table 1. Comparison of source finding time of different algorithms.

Algorithm	Source seeking task				
	1	2	3	4	5
TES	2.37	2.42	2.4	2.36	2.51
TES-DF	2.00	2.03	2.05	2.01	1.93

The statistical results in Table 1 were “actual time consumption/ideal time consumption”, where the actual time consumption referred to the statistical average of 1,000 simulation experiments, and the ideal time consumption referred to the homing time obtained by using the rolling window method along the gradient descent direction under the condition that the surrounding magnetic field distribution was known (note that the homing time consumption was only the ideal value because the surrounding geomagnetic field could not be predicted in advance). The results showed that, in the case of no prior geomagnetic data, the two algorithms could reach the target point with a time ratio less than 3, and both could get rid of the dependence of geomagnetic navigation on the prior database. Among them, the time ratio of TES was approximately 2.4, and the time ratio of TES-DF was about 2. From a statistical point of view, TES-DF improved the homing time ratio by about 17% by suppressing the population drift.

The homing time consumption of 1,000 instances was recorded in Figure 7. From the perspective of homing time consumption, the median line and the position of the rectangular box in the TES-DF plot were lower than those in the TES plot. In other words, TES-DF algorithm could effectively reduce the homing time and improve the navigation search efficiency compared with TES algorithm.

(3) Analysis of key parameters

In TES-DF algorithm, the radius r of the absorbing state could be characterized by the threshold entropy H_{th} , and the two could be approximately regarded as a direct proportion relationship. The population migration speed could be characterized by the change speed of distribution entropy H , which was embodied in the increase of the distribution probability of the new optimal solution through the replication operation, and then the population migrated to the new mature state. The migration speed was determined by the reproduction depth N_{spr} . The effect of threshold entropy on homing search was investigated. According to the previous analysis, the setting of the threshold entropy H_{th} determined the size of the radius r of the attractive domain. Through digital simulation and analysis, the mechanism of the action of threshold entropy on population drift was further explored. Let the sampling interval $D_\theta = 30^\circ$ and the population size $N_{pop} = 50$, selecting multiple values of $H_{th} \in (\min(H), \max(H))$, where $\min(H)$

= 0、 $\max(H) = 2.3$. For each value, 1,000 simulation experiments were carried out, and the homing time was counted. The statistical mean \bar{k} of homing search time consumption under different threshold entropy constraints is shown in the Figure 8.

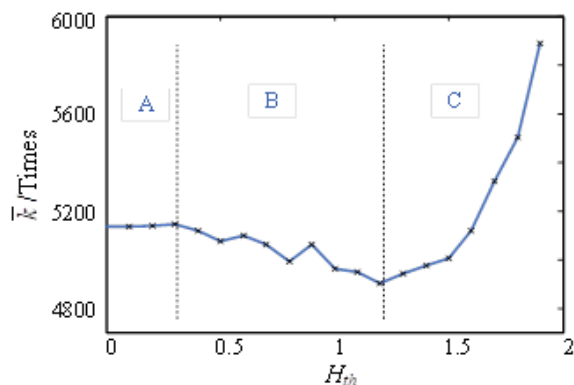


Figure 8. Effects of different threshold entropy H_{th} on the homing time consumption based on TES-DF.

According to the distribution characteristics of \bar{k} , its distribution could be divided into A, B, C three regions. In region A, the threshold entropy was set to $H_{th} < 0.3$. Due to the excessively small value of the threshold entropy in this specific region, it failed to effectively constrain and adjust the homing search process, resulting in negligible changes in homing time. In region B, the threshold entropy was set to $0.3 \leq H_{th} < 1.2$. The threshold entropy imposed constraint on the reduction of population sample types, expanded the radius of attraction region, and thereby achieved the objective of inhibiting population drift and reducing \bar{k} value. In region C, the threshold entropy was set to $1.2 \leq H_{th} < 2$. With the increase of threshold entropy, the radius of the mature state expanded continuously, although the diversity of the population was increased, the population was difficult to converge to the optimal solution, and the \bar{k} value was increased. In contrast, when $H_{th} \in (1.0, 1.5)$, the statistical value of \bar{k} was lower, and when $H_{th} = 1.2$, \bar{k} was taken to the minimum.

The effect of replication depth N_{spr} on homing search behavior was then determined. The term “population migration” refers to the transfer of evolutionary populations between different states, and the velocity of migration has a certain impact on algorithm convergence. The search process based on the TES-DF homing algorithm was characterized by the rate of change of distribution entropy H , which signified the speed at which population migration occurred. This phenomenon was observed through an increase in the distribution probability of the new optimal solution *via* replication operation, resulting in a transition of the population towards a new mature state. The migration speed played a crucial role in facilitating the rapid transition of the population to the new mature state. However, it also posed the risk of local convergence. Conversely, a slow migration speed hampered timely tracking of the solution curve by the algorithm. Notably, the replication depth N_{spr} determined the population's migration speed. By means of digital simulation, the homing effect of copy depth in the range of values was analyzed. The simulation parameter was set as $N_{spr} \in (1, 25)$, and each point position was simulated for 1,000 times. The simulation results of the homing time were shown in Figure 9. The results of the average time spent in all three environments showed that the homing time decreased first and then increased with the increase in N_{spr} (Figure 9a). The time variance $D(k)$ demonstrated that the statistical results and trends of both ideal and noisy environments were highly similar with $D(k) < 0.5 \times 10^6$ (Figure 9b). In the local extreme environment, the time variance showed a large change. In the range of $N_{spr} \leq 5$, the time variance first increased and then decreased with the maximum value over 3.5×10^6 . In the $N_{spr} > 5$ range, the time variance $D(k)$ was around 1×10^6 . If the $N_{spr} \in (1, 4)$ selection was too limited, the migration speed of the population slowed down, resulting in poor information transmission and increasing the time cost of source searching. With the increase in $N_{spr} \in (4, 8)$, the speed of population migration

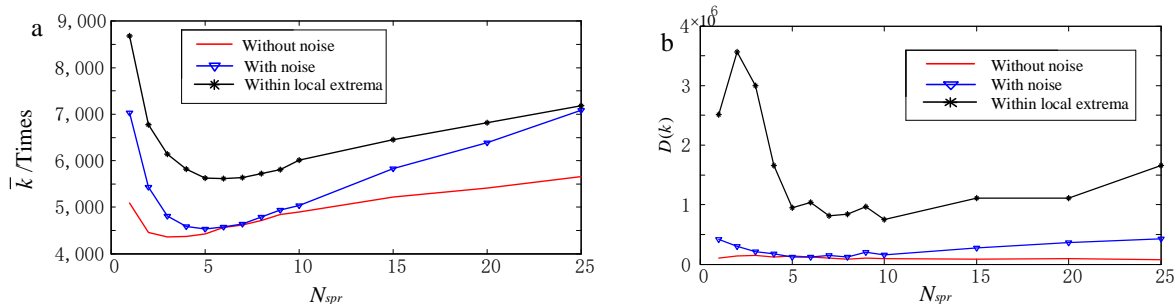


Figure 9. Influence of N_{spr} on homing. **a.** The average of homing time. **b.** The variance of homing time.

was accelerated, enabling the timely tracking of the solution curve by the population. At this stage, satisfactory results were observed in terms of source search time and consistency. When $N_{spr} \in (8, 25)$ continued to increase, rapid population migration resulted in search behaviors that were overly sensitive to environmental changes. Even minor alterations could significantly impact the population and prolong the time required to locate resources. The time spent on source searching was too long at this point, which in turn reduced the variance in time consumption. To enhance the efficiency of the source detection algorithm and integrate its performance across all three environments, it was recommended to opt for propagating operator $N_{spr} \in (4, 8)$.

Conclusion

Aiming at the population drift problem of TES under the constraint of homing path, this study analyzed the action mechanism of each evolutionary operation on population drift, and then proposed a population diversity first (DF) drift suppression strategy from the perspective of expanding the attractive region. TES homing algorithm was improved, and a bio-inspired homing algorithm based on TES-DF was designed. By monitoring the population distribution entropy, the homing algorithm could improve the population diversity as much as possible without affecting the homing search efficiency and achieved the purpose of inhibiting the population

drift. Theoretical analysis and simulation results showed that the improved navigation method could effectively improve the homing efficiency. The results showed that the TES-DF based bionic homing algorithm could effectively suppress the population drift phenomenon and improve the homing efficiency. It was an effective way to reduce the difficulty of population migration by appropriately expanding the radius of attraction region to make the population migration as internal as possible, which could inhibit population drift and improve the dynamic search ability of the algorithm. Replication depth could accelerate swarm migration, but too fast or too slow migration was not conducive to the improvement of homing performance. There are still some shortcomings in this study. The carrier was regarded as a particle, and its motion mechanics was not considered enough in this study, so it should be added later. In the follow-up research, the magnetic field anomaly will also be reflected in the local extremum of the search space, and the effect of its strength, range, and polarity on homing behavior will be analyzed.

Acknowledgements

This work was funded in part by the National Natural Science Foundation of China (Grant No. 62201443) and in part by the Shaanxi Provincial Key Research and Development Plan (Grant No. 2023-YBGY-019) as well as Natural Science Basic Research Program of Shaanxi (Grant No. 2024JC-YBMS-563).

References

1. Ubolsakka-Jones C, Tongdee P, Jones DA. 2019. The effects of slow loaded breathing training on exercise blood pressure in isolated systolic hypertension. *Physiother Res Int.* 24(4):21-31.
2. Denton E, Bondarenko J, O'Hehir RE, Hew M. 2019. Breathing pattern disorder in difficult asthma: Characteristics and improvement in asthma control and quality of life after breathing re-training. *Allergy.* 74(1):201-203.
3. Buehlmann C. 2023. Animal homing: Ants build their own landmarks when they need them. *Curr Biol.* 33(13):R721-R724.
4. Howgego J. 2016. Animal superpowers: How we're homing in on their magnetic satnav. *New Sci.* 229(3065):34.
5. Putman NF. 2020. Animal navigation: Seabirds home to a moving magnetic target. *Curr Biol.* 30(14):R802-R804.
6. Li H, Liu M, Liu K, Zhang F. 2017. A study on the model of detecting the variation of geomagnetic intensity based on an adapted motion strategy. *Sensors.* 18(1):39.
7. Liu M, Liu K, Li H, Li Y. 2014. A study of bio-inspired geomagnetic navigation using timing evolution searching strategy. *Journal of Northwestern Polytechnical University.* 32(6):894-898.
8. Brothers JR, Lohmann KJ. 2015. Evidence for geomagnetic imprinting and magnetic navigation in the natal homing of sea turtles. *Curr Biol.* 25(3):392-396.
9. Brothers JR, Lohmann KJ. 2018. Evidence that magnetic navigation and geomagnetic imprinting shape spatial genetic variation in sea turtles. *Curr Biol.* 28:1325–1329.
10. Iyer A, Benitez-Paez F, Brum-Bastos V, Beggan CD, Demšar U, Long JA, 2022. Spatial-temporal interpolation of satellite geomagnetic data to study long-distance animal migration. *Ecol Inform.* 72(101888):1-16.
11. Kishkinev D, Packmor F, Zechmeister T, Winkler HC, Chernetsov N, Mouritsen H, *et al.* 2021. Navigation by extrapolation of geomagnetic cues in a migratory songbird. *Curr Biol.* 31(7):1562-1569.
12. Monteil CL, Lefevre CT. 2020. Magnetoreception in Microorganisms. *Trends Microbiol.* 28(4):266-275.
13. Winklhofer M. 2019. Magnetoreception: A dynamo in the inner ear of pigeons. *Curr Biol.* 29(32):R1224-R1226.
14. Dora B. 2018. Homing pigeons. *Curr Biol.* 28(17):R966-R967.
15. Ritz T, Wiltschko R, Hore PJ, Rodgers CT, Stapput K, Thalau P, *et al.* 2009. Magnetic compass of birds is based on a molecule with optimal directional sensitivity. *Biophys J.* 96(8):3451-3457.
16. Khan MM, Khan DK. 2020. Bio-motivated geomagnetic navigation based on leading angle technique and parameters. *Advanced Journal of Science and Engineering.* 1(3):69-73.
17. Zein B, Long JA, Safi K, Kölzsch A, Benitez-Paez F, Wikelsk M, *et al.* 2022. Simulating geomagnetic bird navigation using novel high-resolution geomagnetic data. *Ecol Inform.* 69(101689):1-11.
18. Zhou J, Wang Q, Cheng C. 2019. Geomagnetic gradient bionic navigation based on the parallel approaching method. *Proc Inst Mech Eng G J Aerosp Eng.* 233(9):3131-3140.
19. Guo J, Liu M, Liu K, Niu Y. 2020. Research of bio-inspired geomagnetic navigation for AUV based on evolutionary gradient search. *Journal of Northwestern Polytechnical University.* 37(5):865-870.
20. Liu GG, Pei ZY, Liu NX, Tian Y. 2023. Subspace segmentation based co-evolutionary algorithm for balancing convergence and diversity in many-objective optimization. *Swarm Evol Comput.* 83(101410):1-13.